IET Generation, Transmission & Distribution

Research Article

IET Journals
The Institution of Engineering and Technology

Accurate and comprehensive fault location algorithm for two-terminal transmission lines

ISSN 1751-8687
Received on 24th December 2017
Revised 7th July 2018
Accepted on 20th August 2018
E-First on 19th September 2018
doi: 10.1049/iet-gtd.2018.6084
www.ietdl.org

Farhad Poudineh-Ebrahimi[1], Mahdi Ghazizadeh-Ahsaee[1] ✉

[1]*Electrical Engineering Department, Faculty of Engineering, University of Zabol, Zabol, Iran*

✉ *E-mail: ghazizadeh@uoz.ac.ir*

Abstract: In this study, a novel accurate fault location algorithm is presented for two-terminal transmission lines. In contrast to conventional methods, the proposed algorithm not only utilises asynchronous samples recorded during the fault but also needs no line parameters and identification of fault type. In the presented fault-locating method, distributed parameter line model in the time domain and asynchronous data of the terminals collected during fault are applied. Fault locating as an optimisation problem has been solved by the heuristic algorithm of teaching–learning-based optimisation, and the decision variables of fault location, synchronisation time and line parameters are estimated simultaneously. The performance of the presented method was tested with different fault incidence angles, a variety of fault types, and under several system and fault conditions using the MATLAB/Simulink. These tests demonstrate the high accuracy of the presented method. Also, the proposed method did not show any dependence on the impedance of the Thevenin sources of the two sides of the line, the fault impedance and the fault incidence angle. Furthermore, it was not affected by the high resistance of the fault and the network structure.

1 Introduction

There is a constant possibility of fault occurrence in transmission lines. Short circuit faults, which lead to a short- or long-term power outage, may bring huge economic loses for some of the major consumers such as manufacturing industries. Hence, quick return of the system to a normal state is one of the important topics in this regard. The exact determination of the fault location in a line can increase the speed of the line fix, reduce outage time, and thus improve power system reliability [1, 2]. Therefore, an accurate determination of fault point is very important in lines [3–6].

In this connection, several useful methods have been presented for fault locating in the two-terminal transmission lines [5–31]. A group of these methods uses data from one terminal of the line [7–9]. These algorithms depend on Thevenin impedances of both sides, fault incidence angle and fault resistance. To deal with this issue, several algorithms have been presented to work using voltage and current data of both line terminals [10–31]. Also, the methods proposed in [5–23] need precise values of the line parameters for locating the faults. These values may change over the course of time due to various reasons such as different operating conditions, temperature and ground resistivity [24], leading to a reduced accuracy of these methods. Several methods have been proposed to overcome this problem [24–31]. Some methods estimate line parameters using the pre-fault voltage and current information and then apply them in fault locating [25, 26]. Some others calculate the line parameters during the process of fault point determining [24, 27–31]. However, in the methods presented in [24–31], the synchronised voltage and current data sampled during fault were applied. Therefore, in the event of loss of synchroniser signal and thus non-synchronised information, the accuracy of the methods in determining the location of fault will be reduced significantly. Also, the use of synchroniser such as GPS to synchronise sampled data imposes additional costs on the system.

The present study was conducted to determine fault point through a novel method that, unlike conventional methods, not only uses non-synchronous data recorded in the terminals during a fault but also does not require line parameters and does not depend on the shunt fault type. This algorithm uses distributed parameter line model in the time domain and voltage and current samples during the fault directly. The fault-locating process becomes an optimisation problem that can be used for all shunt fault types. The decision variables of this algorithm are the exact location of the fault, the time required for synchronisation and also the line parameters. In other words, information of one line terminal with respect to that of another terminal is delivered to the fault locator with a time delay, with line parameters being unavailable. This method is independent of the Thevenin equivalent impedance of external networks, fault impedance, fault incidence angle, synchronisation angle and shunt fault type. The teaching–learning-based optimisation (TLBO) heuristic algorithm is used to obtain the exact location of the fault.

The remainder of this paper is organised as follows. In Section 2, the basic principle of the proposed fault-locating method for the single-phase transmission line is described and then is generalised to the three-phase transmission line. Section 3 briefly describes the TLBO algorithm. In Section 4, simulations are performed using the MATLAB/Simulink and the results obtained by running the proposed method are presented. Finally, Section 5 gives conclusions.

2 Proposed fault-locating method

Since the proposed fault-locating method is a generalisation of the fault locating for a single-phase transmission line, the principle of the fault-locating algorithm is first described for a single-phase transmission line.

2.1 Fault location for single-phase transmission line

Using the distributed parameter model of the transmission line would lead to a high accuracy of fault locating in long lines because of considering the line capacitance. Fig. 1 shows the single-phase model of a transmission line with distributed parameters in the time domain. In this figure, S and R represent the sending and receiving end of the line, respectively. It is assumed that a fault occurs at a distance of d from the terminal S. Recorded voltage and current samples in the terminals S and R are sent to the fault locator. The data of terminal R are delivered with a time delay of t_{del} relative to the data of terminal S to the fault locator, while line parameters and t_{del} time are considered as unknown.

Fig. 2 shows the distributed parameter line model in the time domain for S-F segment of the transmission line [32]. Using this figure, the following equations can be written:

$$i_S(t+t_{\text{del}}) = \frac{v_S(t+t_{\text{del}})}{z_{sf1}} + I_{FS}(t-\tau) \tag{1}$$

$$i_{FS}(t) = \frac{v_{FS}(t)}{z_{sf1}} + I_{FR}(t-\tau) \tag{2}$$

I_{FS} and I_{FR} are dependent current sources defined as follows:

$$I_{FS}(t) = \frac{R_{SF}}{z_{sf1}^2}[v_S(t+t_{\text{del}}) + z_{sf2} \times i_S(t+t_{\text{del}}) - \frac{Z_C}{z_{sf1}^2}[v_{FS}(t) + z_{sf2} \times i_{FS}(t)] \tag{3}$$

$$I_{FR}(t) = \frac{R_{RF}}{z_{sf1}^2}[v_{FS}(t) + z_{sf2} \times i_{FS}(t) - \frac{Z_C}{z_{sf1}^2}[v_S(t+t_{\text{del}}) + z_{sf2} \times i_S(t+t_{\text{del}})] \tag{4}$$

where v_S and i_S are the voltage and current of the terminal S, respectively; v_{FS} and i_{FS} are the voltage and current at the left-hand side of the fault point, respectively; τ is the wave travel time from the terminal S to the point F.

The parameters in the above equations are defined as

$$R_{SF} = r \times d$$

$$R_{RF} = r \times dr$$

$$z_{sf1} = Z_C + \frac{R_{SF}}{4}$$

$$z_{sf2} = Z_C - \frac{R_{SF}}{4}$$

$$Z_C = \sqrt{\frac{l}{c}}$$

where Z_C is the characteristic impedance of transmission line; dr is the fault distance from the terminal R; l, c and r are the per-unit line length, inductance, capacitance and resistance, respectively.

The relationship between τ and d is as follows:

$$d = \tau \times V_w \tag{5}$$

where V_w is the wave propagation speed along the line.

By removing i_{FS} from (1)–(4), a new equation is obtained. Substituting (5) in the obtained equation, (6) is achieved

$$v_{FS}(t) = \frac{1}{2 \times Z_C^2} \times \left(z_{sf1}^2 \times \left[v_S\left(t + t_{\text{del}} + \frac{d}{V_w}\right) - z_{sf1} \times i_S\left(t + t_{\text{del}} + \frac{d}{V_w}\right)\right] + z_{sf2}^2 \times \left[v_S\left(t + t_{\text{del}} - \frac{d}{V_w}\right) + z_{sf2} \times i_S\left(t + t_{\text{del}} - \frac{d}{V_w}\right)\right] - \frac{z_{sf1}}{4} \times r \times \left[\frac{r}{2 \times z_{sf1}} \times v_S(t+t_{\text{del}}) + 2 \times z_{sf2} \times i_S(t+t_{\text{del}})\right]\right) \tag{6}$$

Similarly, the voltage v_{FR} (right-hand side voltage of the fault point) can be obtained in terms of the voltage and current of the terminal R

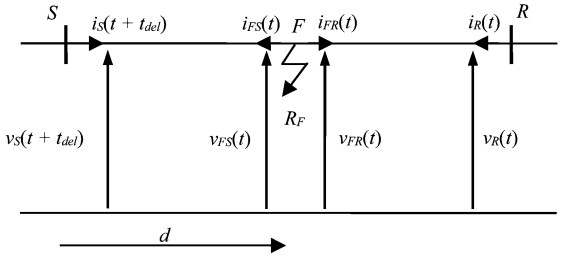

Fig. 1 *Two-terminal transmission line with distributed parameters in the time domain*

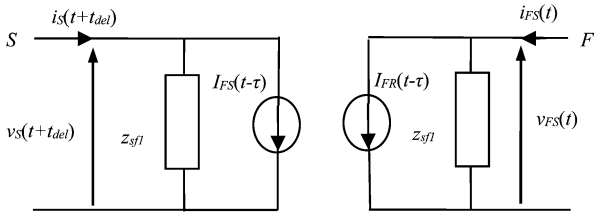

Fig. 2 *Distributed parameters line model for S-F segment*

$$v_{FR}(t) = \frac{1}{2 \times Z_C^2} \times \left(z_{rf1}^2 \times \left[v_R\left(t + \frac{dr}{V_w}\right) - z_{rf1} \times i_R\left(t + \frac{dr}{V_w}\right) + z_{rf2}^2 \times \left[v_R\left(t - \frac{dr}{V}\right) + z_{rf2} \times i_R\left(t - \frac{dr}{V_w}\right)\right] - \frac{z_{rf1}}{4} \times r \times \left[\frac{r}{2 \times z_{rf1}} \times v_R(t) + 2 \times z_{rf2} \times i_R(t)\right]\right) \tag{7}$$

where v_R, i_R are the voltage and current of the terminal R, respectively

$$z_{rf1} = Z_C + \frac{R_{RF}}{4}$$

$$z_{rf2} = Z_C - \frac{R_{RF}}{4}$$

The voltage and current of the terminals are sampled in separate moments. Thus, (6) and (7) should be discretised using the following equation:

$$n = \frac{t}{\Delta t} \tag{8}$$

where Δt is the time interval between two consecutive samples.

The transmission line is continuous and (6) and (7) depend on the values of line parameters and synchronisation angle. Thus, for each registered and available sample set, the v_{FS} and v_{FR} voltages are equal for the real values of line parameters, the correct synchronisation time and the exact location of the fault

$$v_{FS}(n) = v_{FR}(n) \tag{9}$$

Hence, for each available sample set, it is possible to obtain the absolute of the difference between v_{FS} and v_{FR} and then sum them together. In this case, the value of the obtained function for all possible states will be greater than the value of the function for the correct values of its decision variables. Therefore, the following optimisation problem is achieved:

$$g(\mathbf{y}) = \text{Min} \sum_{n=1}^{N} |v_{FS}(n) - v_{FR}(n)|$$

$$\text{Subject to:} \begin{cases} r, l, c > 0 \\ 0 < d < \text{Line length} \\ t_{\text{delmin}} < t_{\text{del}} < t_{\text{delmax}} \end{cases} \tag{10}$$

where $\boldsymbol{y} = [d, t_{\text{del}}, r, l, c]$, $t_{\text{del max}}$, $t_{\text{del min}}$ are the upper and lower limits of synchronisation time, respectively; N is the total number of the available sample sets during a fault.

In (10), there are five decision variables including fault location, synchronisation angle and line parameters. To speed up obtaining these values, function (10) can be minimised via various intelligent optimisation methods [33–35].

By now, the method is presented for single-phase transmission lines, while for three-phase transmission lines it will be developed as follows.

2.2 Fault location for three-phase transmission line

Due to the effect of coupling between phases, the presented method for single-phase case cannot be employed directly for the three-phase case. In the case of the three-phase transmission line, the differential equations of the transmission line in the time domain are interdependent. Therefore, it is necessary to use a suitable real transformation to obtain independent equations [36]. Thus, modal values are obtained as

$$\boldsymbol{v}_{012} = \boldsymbol{M}^{-1} \times \boldsymbol{v}_{ABC} \tag{11}$$

where $\boldsymbol{M}$ is the modal transformation matrix; $\boldsymbol{v}_{ABC} = \begin{bmatrix} v_A \\ v_B \\ v_C \end{bmatrix}$ is the actual voltage matrix in phase domain; $\boldsymbol{v}_{012} = \begin{bmatrix} v_0 \\ v_1 \\ v_2 \end{bmatrix}$ is the voltage matrix in the modal domain; v_A, v_B, v_C are the actual voltage values of phases A, B and C in the phase domain, respectively; v_0, v_1, v_2 are the voltage values in the modal domain.

For actual current values in the phase domain, a similar process must also be done. Three independent modes are obtained by applying modal transformation into the voltage and current matrices in the phase domain. Also, the equations for each mode in the modal domain are separate and in all respects are similar to the single-phase transmission line equation. Therefore, for three-phase lines, an algorithm similar to the single-phase lines can be used. Like the single-phase case, the optimisation function g_m ($m = 0, 1, 2$) can be obtained separately for each mode. Thus, three independent functions are achieved for fault locating

$$g_0(\boldsymbol{y_0}) = \text{Min} \sum_{n=1}^{N} \left| v_{FS}^{(0)}(n) - v_{FR}^{(0)}(n) \right| \tag{12}$$

$$g_1(\boldsymbol{y_1}) = \text{Min} \sum_{n=1}^{N} \left| v_{FS}^{(1)}(n) - v_{FR}^{(1)}(n) \right| \tag{13}$$

$$g_2(\boldsymbol{y_2}) = \text{Min} \sum_{n=1}^{N} \left| v_{FS}^{(2)}(n) - v_{FR}^{(2)}(n) \right| \tag{14}$$

$$\text{Subject to:} \begin{cases} r_k, l_k, c_k > 0, k = 0, 1, 2 \\ 0 < d < \text{Line length} \\ t_{\text{del min}} < t_{\text{del}} < t_{\text{del max}} \end{cases}$$

where $\boldsymbol{y}_k = [d, t_{\text{del}}, r_k, l_k, c_k]$; $v_{FS}^{(k)}$, $v_{FR}^{(k)}$ are the kth mode voltage of left and right side of the fault, respectively.

Each of these functions behaves like function (10), which is used for single-phase transmission line. However, they are not minimised for some states in the correct location. For example, when applying the Karrenbauer transformation [36], considering the obtained transformation matrix, it is seen that mode 1 and mode 2 do not include transient states of C-G fault and B-G fault, respectively. Hence, if mode 1 is used alone, in the event that the C-G fault occurs, the objective function may be minimised at a point other than the fault location. Using mode 2 also does not produce the correct results for B-G fault. On the other hand, mode 0 is inactive for some faults, such as two-phase faults. To overcome this problem, according to the weighted sum method [37], three objective functions are combined to form one optimisation function

$$\begin{aligned} Q(\boldsymbol{u}) &= \text{Min} f \\ f &= \sum_{n=1}^{N} \left| v_{FS}^{(2)}(n) - v_{FR}^{(2)}(n) \right| \\ &\quad + \sum_{n=1}^{N} \left| v_{FS}^{(1)}(n) - v_{FR}^{(1)}(n) \right| \\ &\quad + \sum_{n=1}^{N} \left| v_{FS}^{(0)}(n) - v_{FR}^{(0)}(n) \right| \end{aligned} \tag{15}$$

$$\text{Subject to:} \begin{cases} r_k, l_k, c_k > 0, k = 0, 1, 2 \\ 0 < d < \text{Line length} \\ t_{\text{del min}} < t_{\text{del}} < t_{\text{del max}} \end{cases}$$

where $\boldsymbol{u} = [d, t_{\text{del}}, r_0, l_0, c_0, r_1, l_1, c_1]$.

Notably, since the Q function consists of all three modes, it can be used for all of the symmetric and asymmetric faults and there is no need to detect the type of fault before locating it. This optimisation problem consists of eight decision variables including the fault location, synchronisation time and the values of line sequence parameters. When synchronisation time is achieved, the synchronisation angle can also be calculated. To solve the optimisation problem (15), the algorithm of TLBO is applied. In the following, the summary of this algorithm is presented.

3 Teaching–learning-based optimisation

TLBO [38] is a population-based technique that applies a population of solutions to proceed to the global optimum. This method works on the effect of the influence of a teacher on learners. The population is taken into account as a group of learners or a class of learners. The procedure of TLBO is separated into two portions: the first portion includes the 'teacher phase' and the second one consists of the 'learner phase'. 'Teacher phase' means learning from the teacher while 'learner phase' means learning by the interaction between learners.

3.1 Teacher phase

In teacher phase, teacher will make an effort to shift class mean value towards its own point. So, learner (X_i) modification is achieved as follows:

$$X_{\text{new},i} = X_{\text{old},i} + r_i(M_{\text{new}} - T_F M_i) \tag{16}$$

where M_i is the mean and T_i is the teacher at any iteration i. T_i will make an effort to shift mean M_i towards its own point, therefore now the new mean will be T_i designated as M_{new}. T_F is a teaching factor that decides the value of mean to be modified and r_i is a random amount in the range [0, 1]. The value of T_F can be either 1 or 2, which is also a heuristic step determined randomly with an equal probability as

$$T_F = \text{round}\left[1 + \text{rand}(0, 1)\right]. \tag{17}$$

3.2 Learner phase

A learner learns something new if the other learner has more knowledge than him or her. Learner modification is achieved as follows.

For each i, randomly select two learners X_i and X_j, where $i \neq j$

If $f(X_i) < f(X_j)$

$$X_{\text{new},i} = X_{\text{old},i} + r_i(X_i - X_j) \tag{18}$$

Else

$$X_{\text{new},i} = X_{\text{old},i} + r_i(X_j - X_i) \quad (19)$$

End if

Accept X_{new} if it gives a better function value.

4 Simulation results

To test the efficiency of the proposed algorithm, a three-phase power system including a 300 km transmission line is simulated in MATLAB/Simulink with the specification given in Appendix. The sampling frequency is set to 1 MHz. A data window of half of a cycle is adequate for finding the fault location. It is of note that current transformers, capacitive voltage transformers and analogue anti-aliasing filters are not included in the simulation model. Equation (20) is used to determine the fault-locating error

$$\%\text{ED} = \frac{\text{Calculated distance} - \text{Actual distance}}{\text{Line length}} \times 100\% \quad (20)$$

Equation (21) is also applied to calculate the error percentages of the decision variables values

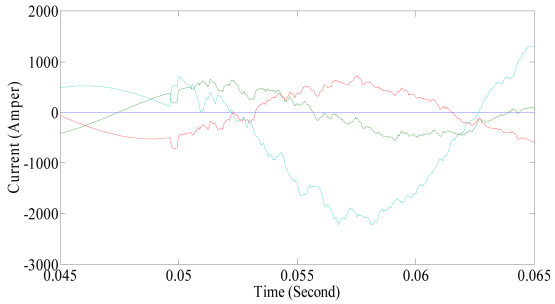

Fig. 3 *Three-phase current of terminal S*

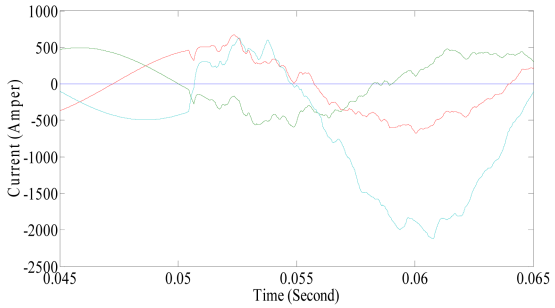

Fig. 4 *Three-phase current of terminal R*

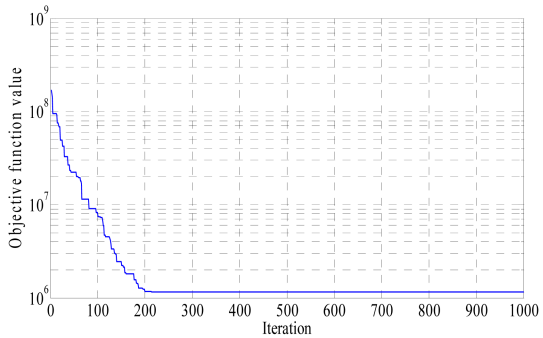

Fig. 5 *Convergence trend of the TLBO algorithm*

$$\%\text{ERLC} = \frac{\text{Calculated value} - \text{Actual value}}{\text{Actual value}} \times 100\% \quad (21)$$

In order to evaluate the proposed algorithm, the time delay is applied to the terminal S data relative to terminal R data. For example, it is assumed that the C-G fault occurs at a distance of 175 km from the terminal S with an incidence angle of 0° and a fault resistance of 10 Ω. Sampled data during the fault are sent to the fault locator. After applying a time delay of 21.6° to samples recorded at the terminal R, the three-phase current waveforms recorded at the terminals S and R are depicted in Figs. 3 and 4, respectively. The fault-locating process is performed by solving (15). For the TLBO, the number of iterations is 1000 and the population size is set to be 100. Fig. 5 illustrates the convergence trend of the algorithm. According to this figure, the TLBO algorithm converges rapidly in few iterations. The percentage of errors related to calculating the fault location and the calculation of the other decision variables are presented in Table 1 for two actual fault distances of 175 and 100 km.

Various evaluations of the proposed algorithm are given below using the TLBO algorithm. These evaluations are reported in Tables 2–7 for different fault types, various values of fault resistance, fault location changes, different values of the fault incidence angle and the synchronisation angle, the variation of the Thevenin impedances of the two ends of the line and measurement errors.

Various faults differently affect the accuracy of the fault location methods. Results of testing the proposed algorithm for different fault types and in different places are presented in Table 2. In this test, the synchronisation angle (θ) is considered to be 21.6°, the fault resistance is 10 Ω and the fault incidence angle is 0°. According to Table 2, it can be seen that the maximum absolute error is about 0.043%, which indicates the high accuracy of the proposed method. These results also show the efficiency of the algorithm for all shunt fault types. The proposed method employs just one optimisation function for all shunt fault types and it is not dependent on the type of fault. In comparison, the algorithm presented in [24] depends on the type of fault and the type of fault must be specified before fault locating.

In order to investigate the effect of the fault resistance on the accuracy of the proposed method, different fault resistances are applied to the test system. The results of the proposed method are presented in Table 3. In these tests, the fault incidence angle is 45° and the synchronisation angle is set to be −15°. The obtained results show the maximum absolute error of about 0.068%, which occurs for an AC fault at 130 km from terminal S. These results indicate the high accuracy of the proposed algorithm.

Also, the incidence angle of the fault affects the transient states of the faults. In order to evaluate the impact of different incidence angles of the fault on the accuracy of the proposed algorithm, various fault incidence angles (0, 45 and 90°) are considered. In this assessment, the synchronisation angle is set to a large value of 90° while the fault resistance is 100 Ω. Moreover, fault distances are 10, 55, 105, 165, 225 and 290 km from terminal S. The results of this assessment are presented in Table 4. As can be seen from this table, the proposed algorithm has a high degree of accuracy for different values of the fault incidence angle and is not sensitive to it.

Since the data of the terminals S and R may be sent asynchronously to the fault locators, methods that use synchronous data of terminals require a synchroniser signal. If this signal is lost, the accuracy of these algorithms will be reduced significantly. However, the method proposed in this paper does not require synchronised data. To verify this claim, the proposed scheme was also tested for several synchronisation angles of 34.6, −34.6, 25,

Table 1 Error percentage corresponding to estimation of decision variables

Actual fault distance, km	d	t_{del}	$r_1 = r_2$	r_0	$l_1 = l_2$	l_0	$c_1 = c_2$	c_0
	%ED		%ERLC					
175	−0.01810	0	0.01565	0.98840	0.0718	0.2317	0.04891	−0.10706
100	3.60×10^{-6}	0	−0.02961	2.15485	0.05949	0.09343	0.03722	0.06435

−25, 100 and −100°. In this study, the fault distance from terminal *S* is 120 km, the fault incidence angle is 120° and the fault resistance is 10 Ω. The results of this assessment are collected in Table 5. These results show well the reliability of the algorithm even at large delay times and indicate no dependence of the proposed method on the synchronisation angle. In comparison, for example in [24], for a small time delay of 0.3 ms (equivalent to a synchronisation angle of 5.4° in the frequency of 50 Hz), the maximum absolute error has been reported 1.307%. In comparison, the method proposed in this paper even at the time delay much

Table 2 Impact of the fault type on the proposed algorithm

Fault type	Actual distance, km				
	10	25	150	260	295
			ED, %		
A-G	−0.00978	−0.02183	-1.29×10^{-12}	0.02012	0.01874
B-G	−0.01194	−0.01839	1.89×10^{-13}	−0.01173	0.00873
C-G	0.02881	−0.02564	9.00×10^{-13}	−0.03912	7.78×10^{-5}
AB-G	−0.00684	−0.02564	6.63×10^{-14}	−0.04305	−0.00615
AC-G	0.02250	0.02430	-4.07×10^{-13}	−0.03015	0.00803
BC-G	−0.01230	−0.02564	2.12×10^{-12}	0.03321	0.00348
AB	−0.01230	−0.03075	1.43×10^{-5}	−0.04305	0.01925
AC	−0.01223	−0.03075	−0.00020	−0.04305	−0.02377
BC	−0.01230	−0.03075	-4.62×10^{-5}	−0.04305	−0.01738
ABC	−0.01230	−0.01518	4.95×10^{-5}	−0.04305	−0.02904
ABC-G	−0.01230	−0.01675	6.35×10^{-5}	−0.04305	−0.01203

Table 3 Impact of the fault impedance on the proposed algorithm

Fault type	Actual fault distance, km	Fault resistance, Ω		
		$R_f = 1$	$R_f = 50$	$R_f = 100$
		ED, %		
C-G	40	−0.02952	0.02562	0.04992
	175	−0.03009	0.00354	−0.02966
	295	−0.01531	−0.00764	−0.00900
BC	45	−0.03690	0.04527	−0.03690
	180	−0.03690	0.04527	−0.03688
	275	−0.06150	−0.05879	−0.03100
AC-G	50	0.05873	2.44×10^{-9}	4.95×10^{-8}
	125	−0.02985	0.00131	0.01745
	250	0.05127	0.02330	0.04210
ABC-G	45	−0.05535	−0.05535	−0.05535
	80	−0.00615	−0.00615	−0.00615
	175	−0.03075	−0.03075	−0.03075
	275	−0.0615	−0.0615	−0.0615
AC	5	−0.00615	−0.00615	−0.00615
	130	−0.06765	−0.06765	−0.06765
	290	−0.06484	−0.01302	−0.00487

Table 4 Impact of the fault incidence angle on the accuracy of the presented method

Fault type	Fault incidence angle, deg	Actual distance, km					
		10	55	105	165	225	290
		Fault location error, %					
ABC-G	0	−0.01230	−0.06765	−0.03690	−0.01845	−0.09055	−0.07995
	45	−0.01230	−0.06765	−0.03690	−0.01845	−0.09055	−0.07995
	90	−0.01230	−0.06765	−0.03690	−0.01845	−0.09055	−0.07995

Table 5 Impact of the synchronisation angle on the accuracy of the proposed method

Fault type	Synchronisation angle					
	$\theta = 34.6°$	$\theta = -34.6°$	$\theta = 25°$	$\theta = -25°$	$\theta = 100°$	$\theta = -100°$
	Error, %					
AB	0.07386	−0.05504	0.07386	−0.05535	0.07386	−0.05535
A-G	0.00728	0.0185	0.01728	0.00522	0.01746	−0.00734
ABC	−0.05535	−0.05535	−0.05535	−0.05535	−0.05535	−0.05535
AB-G	−0.00100	−0.00632	0.01702	−0.02063	0.00613	−0.00816

Table 6 Effect of the source impedance variation on locating the faults with 72° inception angle and 10 Ω fault resistance at 250 km from *S* terminal

Thevenin impedance change, %	In terminal *S*	In terminal *R*	In terminal *S* and *R*
		ED%	
+ 25	0.0262	0.0415	−0.0162
−50	0.0361	0.0153	0.0102
−90	0.0217	0.0113	0.0167
+ 250	0.0273	0.0512	0.0512

Table 7 Effect of measurement errors on locating the faults with 0° inception angle and 100 Ω fault resistance

	Actual distance, km			
Fault type	5	95	195	295
	Fault location error, %			
C-G	−0.00512	−0.01024	0.05686	0.06565
AC	0.08448	0.04829	0.03178	−0.04057
BC-G	−0.00615	−0.02460	0.04615	0.01918

Table 8 Comparison of the capabilities of the proposed method with the existing methods

Algorithm	Maximum absolute error, %	Data	Line parameters	Line model	Source impedances	Fault type
[23]	0.8	Asy	not free	DPTD	free	free
[24]	0.09	Sy	free	DPTD	free	not free
proposed method	0.09	Asy	free	DPTD	free	free

Sy: synchronous; Asy: asynchronous; DPTD: distributed parameter line model in the time domain.

more than this amount (i.e. 100°) has a high degree of accuracy such that the maximum absolute error is well below 0.07%. Thus, this is a step forward to avoid the impact of synchronisation errors and eliminate costs associated with the use of synchroniser signals.

Table 6 presents the impact of changes related to Thevenin impedances of two ends of the line. In this test, AB-G fault has been considered in 250 km from terminal *S*, with a fault resistance of 10 Ω, a fault incidence angle of 72° and a synchronisation angle of −25°. From Table 6, it can be seen that the fault point is obtained with a high accuracy. Therefore, the change in the Thevenin impedances of the two ends of the line has a negligible effect on the accuracy of the presented method.

Data obtained from line terminals may be affected by noise. Accordingly, the error effect of the measured data on the accuracy of the presented method is also studied. For this purpose, it is assumed that the measured data are affected by the noise of −2.5 to + 2.5%. In simulation studies, the fault resistance is 10 Ω, the synchronisation angle (θ) is set to be 40° and the fault incidence angle is 0°. The results of this evaluation are shown in Table 7. As shown in this table, the obtained results confirm the accuracy of the presented algorithm even with the existence of measurement errors.

Given that the distributed parameters line model has been used in the proposed algorithm, it provides a high degree of accuracy for both long and short lines. Also, the proposed algorithm does not need to detect the type of fault before locating the fault. In Table 8, a comparison of the proposed algorithm with previous algorithms is presented. As can be seen, the presented algorithm is a comprehensive one.

5 Conclusion

In this paper, a new precise method is proposed to determine the exact location of a fault in two-terminal transmission lines. This algorithm does not require data synchronisation, availability of line parameters and knowing the shunt fault type. So, the negative effects of synchronisation and line parameters errors on the accuracy of the fault locating are eliminated. The presented method uses the distributed parameters model of the transmission line and samples recorded during the fault directly, while it does not depend on the shunt fault type, Thevenin impedances of both sides of the line, the impedance of the fault and the fault incidence angle. The proposed fault-locating process calculates the fault location, the synchronisation angle and the line parameters by solving just one optimisation function for all shunt fault types. This method is solved using the algorithm of TLBO. Various shunt fault types at different distances and variant conditions were simulated using MATLAB/Simulink. The results of different simulations confirm the high accuracy of the proposed algorithm as the error in all studies is <0.09%.

6 References

[1] Liu, Y., Meliopoulos, A.P.S., Tan, Z., *et al.*: 'Dynamic state estimation-based fault locating on transmission lines', *IET Gener. Transm. Distrib.*, 2017, **11**, (17), pp. 4184–4192

[2] Ghazizadeh-Ahsaee, M.: 'Accurate arcing fault location method for M-terminal transmission lines', *Int. J. Electr. Power Energy Syst.*, 2018, **98**, pp. 147–155

[3] Jin, T., Li, H.: 'Fault location method for distribution lines with distributed generators based on a novel hybrid BPSOGA', *IET Gener. Transm. Distrib.*, 2016, **10**, (10), pp. 2454–2463

[4] Salehi, M., Namdari, F.: 'Fault location on branched networks using mathematical morphology', *IET Gener. Transm. Distrib.*, 2018, **12**, (1), pp. 207–216

[5] Hinge, T., Dambhare, S.: 'Synchronised/unsynchronised measurements based novel fault location algorithm for transmission line', *IET Gener. Transm. Distrib.*, 2018, **12**, (7), pp. 1493–1500

[6] Ghazizadeh-Ahsaee, M., Ghazizadeh-Ahsaee, M., Ghanbari, N.: 'Particle swarm optimization algorithm-based fault location using asynchronous data recorded at both sides of transmission line', *Rev. Roum. Sci. Techn.–Électrotechn. et Énerg.*, 2017, **62**, (2), pp. 148–153

[7] Sadeh, J., Ranjbar, A.M., Hadjsaid, N., *et al.*: 'Accurate fault location algorithm for power transmission lines', *Eur. Trans. Electr. Power*, 2000, **10**, (5), pp. 313–318

[8] Pereira, C., Zanetta, J.: 'Fault location in transmission lines using one-terminal post-fault voltage data', *IEEE Trans. Power. Deliv.*, 2004, **19**, (2), pp. 570–575

[9] Suonan, J., Qi, J.: 'An accurate fault location algorithm for transmission line based on R–L model parameter identification', *Electr. Power. Syst. Res.*, 2005, **76**, pp. 17–24

[10] Kezunovic, M., Mrkic, J., Perunicic, B.: 'An accurate fault location algorithm using synchronized sampling', *Electr. Power Syst. Res.*, 1994, **29**, pp. 161–169

[11] Jiang, J.A., Yang, J.Z., Lin, Y.H., *et al.*: 'An adaptive PMU based fault detection/location technique for transmission lines part I: theory and algorithms', *IEEE Trans. Power Delivery*, 2000, **15**, (2), pp. 486–493

[12] Jiang, J.A., Lin, Y.H., Yang, J.Z., *et al.*: 'An adaptive PMU based fault detection/location technique for transmission lines part II: PMU implementation and performance evaluation', *IEEE Trans. Power Delivery*, 2000, **15**, (4), pp. 1136–1146

[13] Brahma, S.M., Girgis, A.A. 'Fault location on a transmission line using synchronized voltage measurements', *IEEE Trans. Power Delivery*, 2004, **19**, (4), pp. 1619–1622

[14] Samantaray, S.R., Tripathy, L.N., Dash, P.K.: 'Differential equation-based fault locator for unified power flow controller-based transmission line using

synchronised phasor measurements', *IET Gener. Transm. Distrib.*, 2009, **3**, (1), pp. 86–98
[15] Preston, G., Radojević, Z.M., Kim, C.H., *et al.*: 'New settings-free fault location algorithm based on synchronised sampling', *IET Gener. Transm. Distrib.*, 2011, **5**, (3), pp. 376–383
[16] Girgis, A., Hart, D., Peterson, W.: 'A new fault location technique for two- and three-terminal lines', *IEEE Trans. Power Delivery*, 1992, **7**, (1), pp. 98–107
[17] Novosel, D., Hart, D.G., Udren, E., *et al.*: 'Unsynchronized two terminal fault location estimation', *IEEE Trans. Power Delivery*, 1996, **11**, (1), pp. 130–138
[18] Silveira, E.G., Pereira, C.: 'Transmission line fault location using two-terminal data without time synchronization', *IEEE Trans. Power Syst.*, 2007, **22**, (1), pp. 498–499
[19] Liao, Y.: 'Unsynchronized fault location based on distributed parameter line model', *Electr. Power Compon. Syst.*, 2007, **35**, (9), pp. 1061–1077
[20] Izykowski, J., Molag, R., Rosolowski, E., *et al.*: 'Accurate location of faults on power transmission lines with use of two-end unsynchronized measurements', *IEEE Trans. Power Delivery*, 2006, **21**, (2), pp. 627–633
[21] Izykowski, J., Rosolowski, E., Balcerek, P., *et al.*: 'Accurate noniterative fault-location algorithm utilizing two-end unsynchronized measurements', *IEEE Trans. Power Delivery*, 2010, **25**, (1), pp. 72–80
[22] Dalcastagne, A.L., Filho, S.N., Zurn, H.H., *et al.*: 'An iterative two-terminal fault location method based on unsynchronized phasors', *IEEE Trans. Power Delivery*, 2008, **23**, (4), pp. 2318–2329
[23] Ghazizadeh-Ahsaee, M.: 'Accurate NHIF locator utilizing two-end unsynchronized measurements', *IEEE Trans. Power Delivery*, 2013, **28**, (1), pp. 419–426
[24] Davoudi, M., Sadeh, J., Kamyab, E.: 'Parameter-free fault location for transmission lines based on optimisation', *IET Gener. Transm. Distrib.*, 2015, **9**, (11), pp. 1061–1068
[25] Chen, Ch.-Sh., Liu, Ch.-W., Jiang, J.-A.: 'A new adaptive PMU based protection scheme for transposed/untransposed parallel transmission lines', *IEEE Trans. Power Delivery*, 2002, **17**, (2), pp. 395–404
[26] Liao, Y.: 'Online optimal transmission line parameter estimation for relaying applications', *IEEE Trans. Power Delivery*, 2009, **24**, (1), pp. 96–102
[27] Liao, Y., Kang, N.: 'Fault location algorithms without utilizing line parameters based on the distributed parameter line model', *IEEE Trans. Power Delivery*, 2009, **24**, (2), pp. 579–584
[28] Apostolopoulos, C.A., Korres, G.N.: 'A novel algorithm for locating faults on transposed/untransposed transmission lines without utilizing line parameters', *IEEE Trans. Power Delivery*, 2010, **25**, (4), pp. 2328–2338
[29] Liao, Y.: 'Transmission line fault location algorithms without requiring line parameters', *Electr. Power Compon. Syst.*, 2008, **36**, (11), pp. 1218–1225
[30] Elkalashy, N.I.: 'Simplified parameter-less fault locator using double-end synchronized data for overhead transmission lines', *Int. Trans. Electr. Energy Syst.*, 2014, **24**, (6), pp. 808–818
[31] Apostolopoulos, C.A., Korres, G.N.: 'A novel fault-location algorithm for double-circuit transmission lines without utilizing line parameters', *IEEE Trans. Power Delivery*, 2011, **26**, (3), pp. 1467–1478
[32] Dommel, H.W.: 'Digital computer solution of electromagnetic transients in single-and multiphase networks', *IEEE Trans. Power App. Syst.*, 1969, **PAS-88**, (4), pp. 388–399
[33] Venkataraman, P.: '*Applied optimization with MATLAB Programming*' (Wiley, Hoboken, NJ, 2001)
[34] Huang, M.W., Arora, J.S.: 'Optimal design with discrete variables: some numerical experiments', *Int. J Numer. Method Engineering*, 1997, **40**, pp. 165–188
[35] Arora, J.S.: '*Introduction to optimum design*' (Elsevier Academic Press, Boston, 2004)
[36] Johns, A.T., Salman, S.K.: '*Digital protection for power systems*' (Peregrinus, Stevenage, U.K., 1995)
[37] Marler, R.T., Arora, J.S.: 'Survey of multi-objective optimization methods for engineering', *Struct. Multidisc Optim.*, 2004, **26**, pp. 369–395
[38] Rao, R.V., Savsani, V.J., Vakharia, D.P.: 'Teaching–learning-based optimization: a novel method for constrained mechanical design optimization problems', *Comput.-Aided Des.*, 2011, **43**, pp. 303–315

7 Appendix

Power system specifications:

System nominal voltage: 245 kV;
System nominal frequency: 60 Hz;
Phase angle between voltage sources: 20.

Transmission line parameters:

Positive and negative sequence:

$R_1 = 0.0275\ \Omega$/km;
$L_1 = 1.002768$ mH/km;
$C_1 = 13$ nF/km.
Zero sequence:

$R_0 = 0.275\ \Omega$/km;
$L_0 = 3.4505998$ mH/km;
$C_0 = 8.5$ nF/km.